

Comparative Ploidy Proteomics of *Candida albicans* Biofilms Unraveled the Role of the *AHP1* Gene in the Biofilm Persistence Against Amphotericin B*

Thuyen Truong[‡], Guisheng Zeng[§], Lin Qingsong[¶], Lim Teck Kwang[¶], Cao Tong[‡], Fong Yee Chan[§], Yue Wang^{§**}, and Chaminda Jayampath Seneviratne^{‡**}

Candida albicans is a major fungal pathogen causing lethal infections in immunocompromised patients. *C. albicans* forms antifungal tolerant biofilms contributing significantly to therapeutic failure. The recently established haploid *C. albicans* biofilm model provides a new toolbox to uncover the mechanism governing the higher antifungal tolerance of biofilms. Here, we comprehensively examined the proteomics and antifungal susceptibility of standard diploid (SC5314 and BWP17) and stable haploid (GZY792 and GZY803) strains of *C. albicans* biofilms. Subsequent downstream analyses identified alkyl hydroperoxide reductase 1 (*AHP1*) as a critical determinant of *C. albicans* biofilm's tolerance of amphotericin B. At 32 $\mu\text{g/ml}$ of amphotericin B, GZY803 haploid biofilms showed 0.1% of persister population as compared with 1% of the diploid biofilms. *AHP1* expression was found to be lower in GZY803 biofilms, and *AHP1* overexpression in GZY803 restored the percentage of persister population. Consistently, deleting *AHP1* in the diploid strain BWP17 caused a similar increase in amphotericin B susceptibility. *AHP1* expression was also positively correlated with the antioxidant potential. Furthermore, *C. albicans ira2 Δ/Δ* biofilms were susceptible to amphotericin B and had a diminished antioxidant capacity. Interestingly, *AHP1* overexpression in the *ira2 Δ/Δ* strain restored the antioxidant potential and enhanced the persister population

against amphotericin B, and shutting down the *AHP1* expression in *ira2 Δ/Δ* biofilms reversed the effect. In conclusion, we provide evidence that the *AHP1* gene critically determines the amphotericin B tolerance of *C. albicans* biofilms possibly by maintaining the persisters' antioxidant capacity. This finding will open up new avenues for developing therapies targeting the persister population of *C. albicans* biofilms. The mass spectrometry proteomics data are available via ProteomeXchange with identifier PXD004274. *Molecular & Cellular Proteomics* 15: 10.1074/mcp.M116.061523, 3488–3500, 2016.

Candida albicans is a major commensal fungal species in the human microbiota, which inhabits nearly 70% of healthy individuals (1). However, *C. albicans* transforms into an opportunistic pathogen in compromised host populations and accounts for ~15% of healthcare infections with associated mortality as high as 40% (2–4). Ability to form surface-attached microbial communities or biofilm formation is a prominent virulence attribute of *C. albicans* (5, 6). Biofilms of *C. albicans* often develop on medical indwelling devices, producing dormant persister populations that largely contribute to the multidrug tolerance of biofilms (6, 7). Hence, biofilm growth of *C. albicans* is directly linked with therapeutic failure, which causes severe consequences to the host.

The higher antifungal resistance of *C. albicans* biofilms is well documented (6, 8). Although various hypotheses have been proposed to explain the higher resistance in the biofilm mode of growth, the mechanism is still poorly understood (9). In the present study, we took advantage of the recently discovered haploid strains of *C. albicans* (10) to uncover the mechanism behind the higher persistence of the *C. albicans* biofilms against amphotericin B, a drug known as “gold-standard” antifungal agent (11). We previously developed an efficient molecular method to generate mutants from haploid *C. albicans* (12) and used a novel haploid biofilm model of *C. albicans* to unravel a novel biofilm regulator (13).

In this study, we comprehensively conducted comparative ploidy proteomics and antifungal susceptibility tests of diploid

From the [‡]Oral Sciences, Faculty of Dentistry, National University of Singapore, Singapore 119083, the [§]Institute of Molecular and Cell Biology, Agency for Science, Technology and Research, Proteos, Singapore 138673, and the [¶]Department of Biological Sciences, Faculty of Science, National University of Singapore, Singapore 117543

Received June 5, 2016, and in revised form, September 16, 2016

Published, MCP Papers in Press, September 22, 2016, DOI 10.1074/mcp.M116.061523

Author contributions: C. J. S., and Y. W. conceived, designed, provided general guidance, and co-wrote the manuscript. T. T. performed the biofilm experiments, protein extractions, proteomics analysis, and co-wrote the manuscript. G. Z. constructed most of the yeast strains, performed the western blot, and co-wrote the manuscript. L. Q., and L. T. K. conducted the mass spectrometry, gave advices to the proteomics analysis, and revised the manuscript. C. T. gave guidance and assisted in the biofilm experiments. F. Y. C. assisted strain construction and western blot analysis.

and haploid *C. albicans* biofilms using two standard diploid strains, SC5314 and BWP17 and two stable haploid strains, GZY792 and GZY803. Subsequently, downstream analyses led us to identify *AHP1* as a critical determinant of amphotericin B tolerance in the surviving cell population of *C. albicans* biofilms. Using targeted genetic approaches, we obtained new mechanistic insights about the role of *AHP1* in determining the resistance of *C. albicans* biofilms against amphotericin B.

EXPERIMENT PROCEDURES

Fungal Strains and Culture Conditions—Two diploids, SC5314 and BWP17, and two stable haploids, GZY792 and GZY803, were used as standard *C. albicans* diploid and haploid strains. The constructions of yeast strains and plasmids used in this study are described in [supplemental Table S1](#). Fungal cells were cultured at 30 °C in YPD (2% yeast extract, 1% peptone, and 2% glucose), or GMM (glucose minimal medium, 6.79 g/l yeast nitrogen base without amino acids, and 2% glucose) supplemented with appropriate amino acids (uridine 80 µg/ml, arginine 40 µg/ml, and histidine 40 µg/ml) if necessary. Solid culture plates were prepared by the addition of 2% agar.

Antifungal Agents—Amphotericin B, Caspofungin, Fluconazole, Ketoconazole, and Voriconazole (Sigma-Aldrich, St. Louis, MO) were used in this study.

Biofilm Formation—Biofilm development methodology was adapted from our well-established protocol (13, 14). For each strain, single colonies were inoculated in liquid GMM supplemented with required amino acids and incubated at 30 °C overnight. The cultures were then used to prepare cell suspension of MacFarland of 0.375 (equivalent to 10⁷ cell/ml). An aliquot of 100 µl of the suspension was put in one well in a sterile flat bottom 96-well plate (Greiner bio-one). The plates were incubated at 37 °C for 1.5 h with the shaking speed of 80 rpm. After this adhesion phase, non-adhered cells were removed and 200 µl of fresh GMM were added to the adhered cells. The plates were incubated at 37 °C till 72 h; media were changed every 24 h to remove nonadhered cells.

Quantification of Biofilms by XTT and Colony Forming Unit Methods—Biofilms were quantified using 2, 3-bis (2-methoxy-4-nitro-5-16 sulfophenyl)-5-[(phenylamino) carbonyl]-2H-tetrazolium hydroxide (XTT) reduction assay and/or colony forming unit (CFU) counting method as previously described (13). For XTT assay, biofilms were incubated with XTT solution (4 µM of menadione and 0.2 mg/ml of XTT in PBS) at 37 °C and kept in dark for 20 min. Solutions were then transferred to a new 96-well plate and colorimetric changes were measured at 490 nm using a calibrated spectrophotometer (Multiskan™ GO, Thermo Scientific, Waltham, MA). For CFU assay, serial dilutions were performed on biofilm suspension and spread onto Sabouraud dextrose agar (SDA) plates to incubate at 30 °C for 48 h before counting the colonies.

Antifungal Susceptibility Testing for Planktonic *C. albicans* Cells—Determination of minimum inhibition concentration (MIC)¹ was performed according to the Clinical and Laboratory Standards Institute (CLSI) guideline (15). Briefly, overnight *C. albicans* cultures at 30 °C in GMM supplemented with required amino acids were used to prepare a cell suspension of 0.38 McFarland standard (equivalent to 10⁷ cells/ml). The suspension was diluted with RPMI to yield an inoculum of ~0.5 × 10³ to 2 × 10³ cells/ml. The MIC was performed in 96-well

plate platform and each strain was exposed to the 2-fold diluted solutions of the mentioned antifungals. The plates were incubated at 30 or 37 °C for 48 h before MIC values were recorded following the guideline. In order to obtain comparable planktonic MIC to that of the biofilm mode, additional Antifungal susceptibility testing was performed with the final inoculum of 10⁷ cells/ml as we have previously described (14).

Antifungal Susceptibility Testing for *C. albicans* Biofilm—Antifungal susceptibility testing for *C. albicans* biofilm was conducted via XTT method or CFU assay. After 72 h biofilm formation, media were removed and cells were incubated in different antifungal concentrations in RMPI. The plates were incubated at 37 °C for 24 h. XTT methods or CFU assays were performed as described above to estimate the biofilm susceptibility. For survival rate at 32 µg/ml amphotericin B, statistical analysis was performed using analysis of variance. Differences were considered significant when *p* values are less than 0.05.

Antioxidant Capacity Assay—Seventy-two-hour biofilm cells were collected in lysis buffer (50 mM Tris-HCl pH 7.4, 150 mM KCl, 1% Nonidet P-40). Samples were homogenized using glass beads (0.5 mm) and a high speed vortex (Vortex-genie, Scientific Industries, Bohemia, NY) following 7 cycles of 1 min on and 2 min off ice. Total antioxidant capacity assay kit (Abcam, Cambridge, MA) was used to estimate the total antioxidant potentials of the biofilms following manufacture protocol. Statistical analysis was performed using analysis of variance. Differences were considered significant when *p* values are less than 0.05.

RNA Extraction and Real-time PCR—RNA was extracted from 72 h biofilms cells using TRIzol following the manufacture's protocol (Invitrogen, Carlsbad, CA). RNA was used for reverse transcription (Promega, Singapore) and real-time PCR (KAPA biosystem) was performed to estimate the level of RNA of interests. Primer sequences for real-time PCR were adapted from previous publication (16, 17). Statistical analysis was performed using analysis of variance. Differences were considered significant when *p* values are less than 0.05.

Protein Extraction and Western Blot—Biofilm cells were harvested into 2-ml screw-cap microcentrifuge tubes, washed once by PBS, and resuspended into 9 M urea lysis buffer (20 mM HEPES [pH8.0], 9 M urea, 1 mM sodium orthovanadate, 2.5 mM sodium pyrophosphate, 1 mM β-glycerophosphate). After addition of acid-washed glass beads (Sigma-Aldrich), cells were broken by six rounds of 60-s beating at 5000 rpm in a MicroSmash MS-100 beater (TOMY Medico, Tokyo, Japan) with 1 min of cooling between rounds. The lysed cells were then centrifuged at 16,000 rpm for 15 min at RT. Supernatants were then collected and the protein concentrations were determined by Nanodrop 1000 (Thermo scientific). After mixed with 3× protein loading buffer (150 mM Tris-HCl, pH 6.8, 6% SDS, 30% glycerol, 3% β-mercaptoethanol, 37.5 mM EDTA, 0.06% bromphenol blue), normalized protein samples (100 µg) were separated by SDS-PAGE and subsequently transferred to a PVDF membrane (Bio-Rad Laboratories, Hercules, CA). For Western blot analysis, the membrane was first incubated with 5% BSA (dissolved in PBS containing 0.1% Tween-20, PBST) at room temperature for 1 h (or at 4 °C overnight). After a brief rinse with PBST, the membrane was incubated with PBST containing a 1:2500 diluted first antibody (mouse monoclonal Myc antibody, Nacalai Tesque, Tokyo, Japan) at RT for 1 h, followed by three rounds of 5-min wash with PBST. The membrane was then incubated with PBST containing a 1:5000 diluted secondary antibody (HRP-linked anti-mouse IgG from sheep; GE Healthcare UK). After three rounds of 5-min wash with PBST, the membrane was immersed in Pierce ECL WB substrate solution (Thermo Scientific) and exposed to X-film (Fujifilm). Next, the membrane was stripped with Restore Western blot Stripping Buffer (Thermo Scientific) as instructed by the manual and blocked with 5% BSA again. Subsequently, the mem-

¹ The abbreviations used are: MIC, minimum inhibition concentration; AHP1, alkyl hydroperoxide reductase 1; IRA2, Inhibitory Regulator of the RAS-cAMP pathway; iTRAQ, Isobaric tags for relative and absolute quantitation.

brane was reprobed with 1:2500 diluted first antibody PSTAIRE (Santa Cruz Biotechnology, Dallas, TX) and 1:2500 diluted secondary antibody (HRP-linked anti-rabbit IgG from goat; Santa Cruz Biotechnology) to detect the house keeping protein Cdc28.

Protein Extraction for iTRAQ Analysis—Seventy-two-hour biofilms of SC5314, BWP17, GZY792, and GZY803 were taken for protein extraction. Biofilm was washed once with PBS and cell pellets were solubilized in triethylammonium bicarbonate (TEAB)/urea/triton-X/SDS (TUTS) buffer. Samples were homogenized using glass bead (0.5 mm) in an Omni Bead rupter 24 (Omni International Inc., Kennesaw, GA) following operator protocol. Lysates were collected and protein concentration was determined using Bradford assay (Bio-Rad).

In-Solution Digestion and Samples Clean Up—For each sample, 100 μ g of proteins were taken. Solution was diluted with 0.5 M TEAB to a SDS concentration of less than 0.05%; pH was adjusted to 8. Subsequently, samples were reduced with 5 mM TCEP at 65 °C for 60 min and alkylated with 10 mM MMTS for 15 min at room temperature. Following reduction and alkylation, 1 μ g of trypsin per 20 μ g of proteins were added and trypsinization was performed at 37 °C for 16 h. Digested peptides were stored at -20 °C before LC separation and MS analysis. Samples were then acidified and subjected to strong cation-exchange chromatography using iTRAQ method development kit (SCIEX, Foster City, CA). Elutes were then desalted in Sep-Pak C18 cartridge (Waters, Milford, MA), dried, and then reconstituted in 25 μ l of diluent (98% water, 2%ACN, and 0.05% formic acid) before sending for LC-MS/MS analysis.

LC-MS/MS Analysis—The detailed methodology for LC-MS/MS has been previously described by our group (18). In brief, the peptides were dissolved with 50 μ l mobile phase A (2% acetonitrile, 0.1% formic acid). Water peptide separation was conducted using an Eksigent nanoLC Ultra and ChiPLC-nanoflex (Eksigent, Dublin, CA) in TrapElute configuration. Samples were then loaded on a 200 μ m \times 0.5 mm column and eluted on an analytical 75 μ m \times 15 cm column (ChromXP C18-CL, 3 μ m). An amount of 2 μ l of the sample was separated by a gradient formed by mobile phase A (2% acetonitrile, 0.1% formic acid) and mobile phase B (98% acetonitrile, 0.1% formic acid) at 3 μ l/min flow rate. The following gradient elution was used for peptide separation: 5 to 5% of mobile phase B in 1 min, 5 to 12% of mobile phase B in 15 min, 12 to 30% of mobile phase B in 104 min, 30 to 90% of mobile phase B in 2 min, 90 to 90% in 7 min, 90 to 5% in 3 min, and finally held at 5% of mobile phase B for 13 min. The tandem MS analysis was performed using a 5600 TripleTOF system (SCIEX) under Information Dependent Mode. The mass range of 400–1800 m/z and accumulation times of 250 ms per spectrum were chosen for precursor ions selections. MS/MS analysis was performed on the 20 most abundant precursors (accumulation time: 100 ms) per cycle with 15 s dynamic exclusion. Recording of MS/MS was acquired under high sensitivity mode with rolling collision energy.

Protein Identification and Quantification—Peptide identification and quantification was carried out on the ProteinPilot 4.5 software Revision 1656 (AB SCIEX) using the Paragon database search algorithm (4.5.0.0.1654) and the integrated false discovery rate (FDR) analysis function. The data were searched against a protein sequence database downloaded from UniProtKB for *C. albicans* SC5314 on 25th May, 2015 (total 14,851 entries). The MS/MS spectra obtained were searched using the following user-defined search parameters: Sample Type: iTRAQ 8-plex (Peptide Labeled); Cysteine Alkylation: MMTS; Digestion: Trypsin; Instrument: TripleTOF5600; Special Factors: None; Species: None; ID Focus: Biological Modification; Database: Algae Transcriptome.fasta; Search Effort: Thorough; FDR Analysis: Yes; The MS/MS spectra were searched against a decoy database to estimate the false discovery rate (FDR) for peptide identification. The decoy database consisted of reversed protein sequences from the *C. albicans* database. The resulting data set was

auto bias-corrected to remove any variations imparted because of the unequal mixing during the combination of different labeled samples. Different modification states of the same peptide sequences are considered distinct by the software. In this study, a strict unused score cut-off ≥ 1.3 was adopted as the qualification criterion, corresponding to a peptide confidence level of $\geq 95\%$. The identified proteins with ≥ 2 peptides corresponding to 95% confidence interval were selected and further filtered using population statistics (19). Population statistic was also applied to select the cut-off for up-regulated and down-regulated proteins. Protein expression profiling of haploid biofilms was also clustered using Cluster (version 3.0) and Treeview (version 1.1.6) software (20).

Gene Ontology Analysis—Identified proteins were subjected to gene ontology analysis using Cytoscape (v2.8.3) (21) with BINGO plugin (v2.44) (22). Figures generated were abstracted from Cytoscape as previously described (23).

Experimental Design and Statistical Rationale—Seventy-two-hour *C. albicans* haploid and diploid biofilms were collected for iTRAQ-based mass spectrometry analysis. Two haploid (GZY792 and GZY803) and two diploid strains (SC5314 and BWP17) were used as haploid and diploid replicates, respectively. Two biofilm samples of each strain under identical environmental conditions were obtained as the technical replicates. In order to obtain a proteomic expression data set in *C. albicans* haploid biofilms, independent of strain variation, cross comparison was performed between biofilm proteomes of the two haploid strains and those of the two diploid strains (Fig. 1). In other words, proteins that were similarly expressed in all four strains were considered “common” for the biofilm proteome of *C. albicans*. The proteins that were differentially expressed between haploid and diploid biofilm proteomes were classified as “distinctly expressed.” For other biochemical, functional, and quantitative assays, such as transcriptional analysis, XTT and CFU quantitative methods, and total antioxidant capacity estimation, one representative haploid strain, GZY803, was examined and normalized to that of a diploid control strain, BWP17. Experiments were performed in at least three biological replicates and significance of the results was analyzed following analysis of variance. Differences were considered significant when *p* values are less than 0.05.

RESULTS

iTRAQ-based Quantitative Proteomics of Haploid and Diploid Biofilms of *Candida albicans*—To understand the molecular mechanism operating in the biofilm mode of growth of *C. albicans* haploids, we performed an iTRAQ-based mass spectrometry (24) profiling of proteins of 72 h mature biofilms of the two haploids, GZY792 and GZY803 compared with that of the diploids, SC5314 and BWP17. The methodology that was used to analyze the changes in protein expression among different biofilm samples is illustrated in [supplemental Fig. S1](#). Using a decoy database search strategy, FDRs for protein and peptides were estimated as 2.8% and 0.4%, respectively. From the search results, a cutoff of protein unused score ≥ 1.3 (corresponds to 95% confidence) was used as qualification criterion, which resulted in 511 proteins. No protein or peptide identified from the decoy database had $\geq 95\%$ confidence based on our ProteinPilot search result. Among the proteins that satisfied the stringent cutoff of protein unused score ≥ 1.3 , 374 proteins identified by more than one single peptide were selected for further study. Cross comparison was performed between biofilm proteomes of the two haploid and

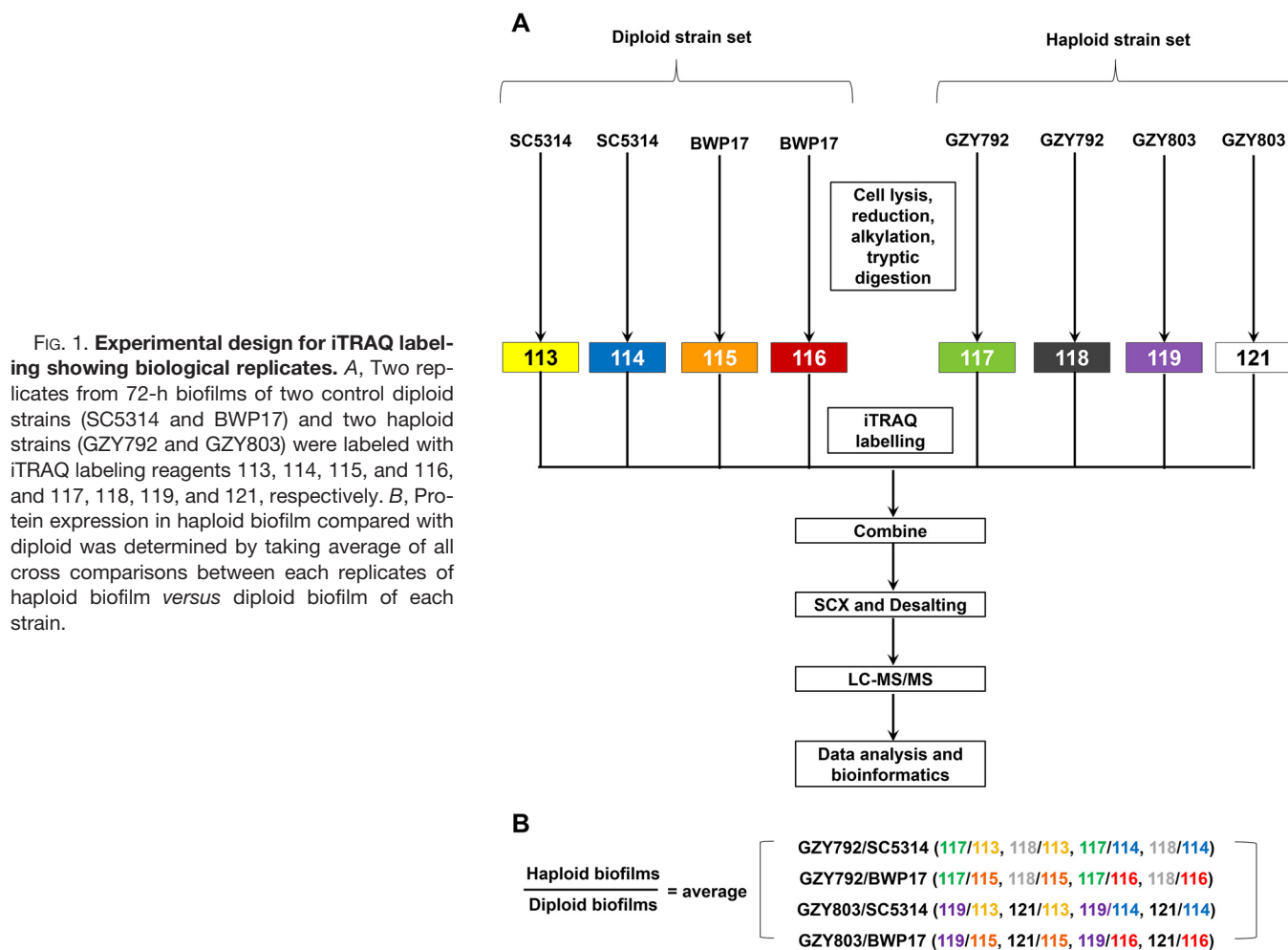


FIG. 1. Experimental design for iTRAQ labeling showing biological replicates. A, Two replicates from 72-h biofilms of two control diploid strains (SC5314 and BWP17) and two haploid strains (GZY792 and GZY803) were labeled with iTRAQ labeling reagents 113, 114, 115, and 116, and 117, 118, 119, and 121, respectively. B, Protein expression in haploid biofilm compared with diploid was determined by taking average of all cross comparisons between each replicates of haploid biofilm *versus* diploid biofilm of each strain.

two diploid strains. Ratio of protein expression of haploid relative to diploid biofilms was estimated as average of each cross comparison (Fig. 1). Subsequently, deviation of ratios (*i.e.* 117/113) of individual proteins between various replicates was calculated as described previously (25). Geometric mean, standard deviation and percentage coefficient of variation (%CV) of 374 proteins were also determined. Next, to determine cutoff threshold, population statistical analyses (19) were applied which showed that %CV = 66% corresponded to 88% coverage of the data; therefore, the cut-off fold was fixed at 1.66-fold (66%) for increased, and 0.6-fold (1/1.66) for decreased proteins (supplemental Fig. S2). On the other hand, from the original 374 proteins, 39 proteins that showed large variation between haploid and diploid samples, indicated by % CV larger than 66% were filtered out. Thereafter, student-*t* statistical test was applied to the remaining 335 proteins. Expression was considered significant when *p* value was less than 0.05 between samples. Applying the cutoff threshold determined by population statistics (supplemental Fig. S2) to these significantly altered proteins resulted in 55 significantly increased proteins and 45 significantly decreased proteins (Fig. 2A). Hence, 235 remaining proteins were then classified

as the common proteins between the haploid and diploid biofilms (Fig. 2A). Expression pattern of these proteins was also illustrated and organized by two-dimensional hierarchical clustering (Fig. 2B). Each protein was colored corresponding to its fold change. In addition, pathway analysis by Cytoscape (21) revealed that similarly expressed proteins were mapped into the pathways of nucleoside and protein metabolism, protein and metabolite precursor generation, co-factor binding, and cellular and ribosomal structures (Fig. 2C). On the other hand, mapping differently regulated proteins to their gene ontology revealed that nucleoside biosynthesis, dicarboxylic acid metabolism, cellular respiration, and ATP synthesis-coupled proton transport were significantly increased; and, nucleoside breakdown, glycolysis, cell wall and ribosomal proteins expression were suppressed in the haploid biofilm proteome as compared with the diploids (Fig. 2D, 2E, and supplemental Table S2). Full lists of similarly and distinctively expressed proteins between haploid and diploid biofilms are given in supplemental Table S3. In addition, to examine the reliability of our results, we confirmed expression of selected genes at the transcriptional level using real time PCR (supplemental Fig. S3).

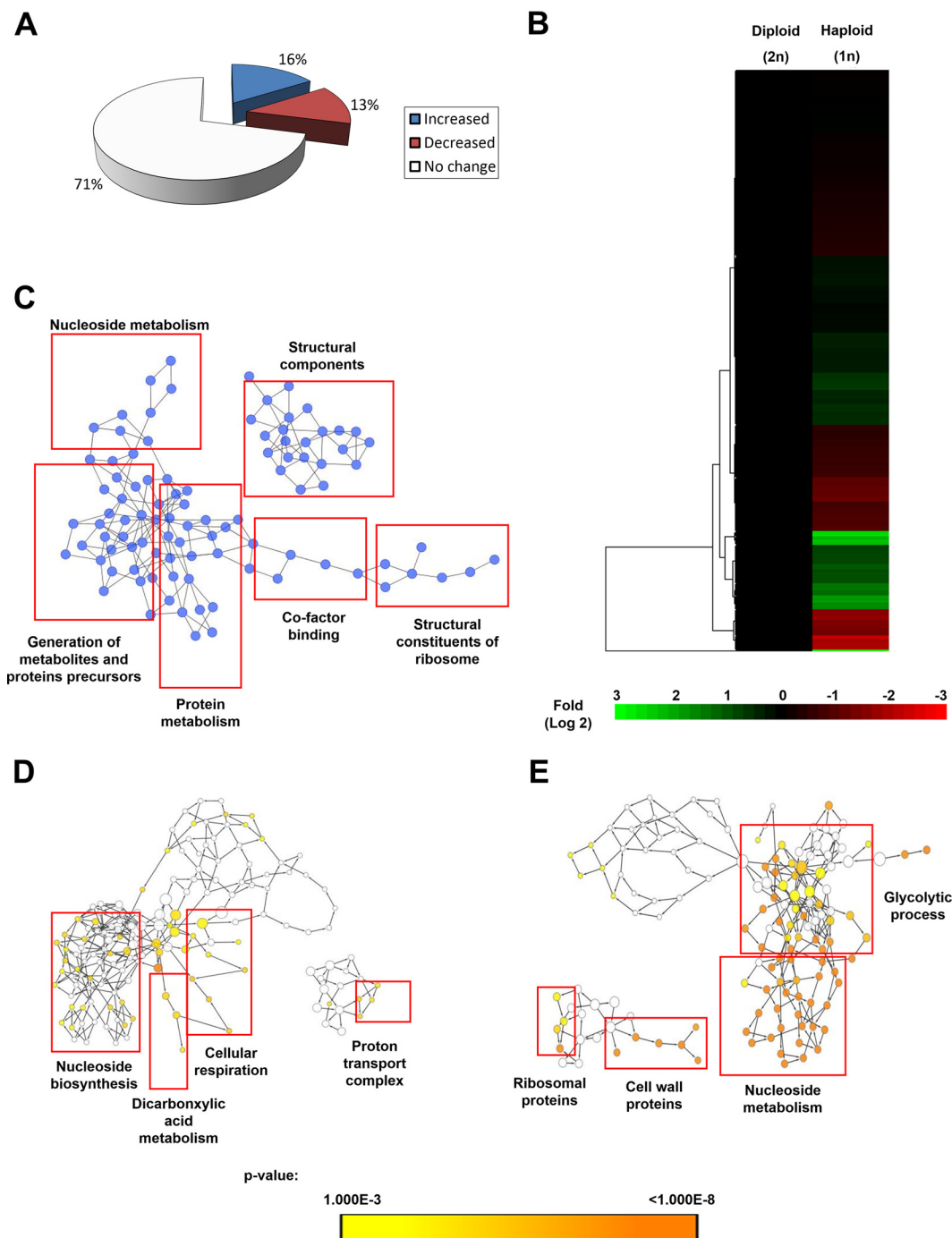


FIG. 2. Protein expression function classification of 72 h haploid versus diploid *C. albicans* biofilms. Two commonly used *C. albicans* diploids (SC5314 and BWP17) and two standard haploids (GZY792 and GZY803) were used in this study. Fungal cells cultured overnight at 30 °C in GMM (supplemented with required amino acids) were used to allow biofilm development at 37 °C. Proteins from 72-h biofilms were extracted and processed for iTRAQ mass spectrometry. *A*, Percentage of similarities and differences in proteomes of haploid compared with diploid biofilm were represented. *B*, Clustered display of haploid biofilms' protein expression profiles as normalized to diploids generated using Cluster and Tree view software. *C*, Biological processes, molecular functions, and cellular components that are similarly regulated in haploid and diploid biofilms. Biological processes, molecular functions, and cellular components that are significantly higher (*D*) and lower (*E*) in the haploid compared with the diploid biofilm.

Comparative Antifungal Susceptibility of C. albicans Haploid and Diploid Biofilms—Analysis of the proteomic data showed differential proteomics responses between haploid

and diploid biofilms, providing information that may explain the phenotypic differences between the two types of *C. albicans* cells (26–28). To further examine the differential behav-

TABLE I

Antifungal susceptibility of *C. albicans* in different modes of growth. Two commonly used *C. albicans* diploids (SC5314 and BWP17) and two standard haploids (GZY792 and GZY803) were used in this study. Fungal cells cultured overnight at 30 °C in GMM (supplemented with required amino acids) were used to prepare the required inoculum for the antifungal susceptibility test. Minimum inhibition concentration (MIC) was recorded by following the CLSI guideline, or optical density (planktonic), or XTT test (biofilm cells)

Strains	MIC ($\mu\text{g/ml}$)				
	30 °C		37 °C		Biofilm $10^7/\text{ml}$
	CLSI $10^3/\text{ml}$	Planktonic $10^7/\text{ml}$	CLSI $10^3/\text{ml}$	Planktonic $10^7/\text{ml}$	
Amphotericin B					
SC5314	0.25	0.5	0.25	0.5	16
BWP17	0.25	0.5	0.25	0.5	16
GZY792	0.25	0.5	0.25	0.5	2
GZY803	0.25	0.5	0.25	0.5	2
Caspofungin					
SC5314	0.5	2	0.5	2	>32
BWP17	0.5	2	0.5	2	>32
GZY792	0.5	2	0.5	2	>32
GZY803	0.5	2	0.5	2	>32
Fluconazole					
SC5314	0.5	2	0.25	2	>32
BWP17	0.5	2	0.25	2	>32
GZY792	0.25	2	0.25	2	>32
GZY803	0.25	2	0.25	2	>32
Ketoconazole					
SC5314	0.125	0.25	0.125	0.25	>32
BWP17	0.125	0.25	0.125	0.25	>32
GZY792	0.125	0.25	0.125	0.25	>32
GZY803	0.125	0.25	0.125	0.25	>32
Voriconazole					
SC5314	0.006	0.06	0.006	0.06	>32
BWP17	0.006	0.06	0.006	0.06	>32
GZY792	0.006	0.06	0.006	0.06	>32
GZY803	0.006	0.06	0.006	0.06	>32

ior, we performed antifungal susceptibility tests on *C. albicans* haploid and diploid strains in the planktonic and biofilm modes using standard micro-dilution assays (14). In the planktonic mode, *C. albicans* haploids showed a similar susceptibility as the diploids to all antifungals tested (Table I). In addition, the haploids in the biofilm mode exhibited higher resistance to the antifungals tested including caspofungin, fluconazole, ketoconazole, and voriconazole, similar to the biofilms of diploids (BWP17). Intriguingly, the haploid biofilm was more susceptible to amphotericin B than the diploid biofilm. This observation was further confirmed by counting colony forming units (CFU) (Fig. 3A). The minimum inhibitory concentration (MIC) of the haploid GZY803 biofilms against amphotericin B was 2 $\mu\text{g/ml}$ whereas that of the diploid BWP17 biofilm was 16 $\mu\text{g/ml}$. At amphotericin B concentration of 2 $\mu\text{g/ml}$, less than 10% of GZY803 biofilm cells survived the treatment as compared with the untreated control. On the contrary, 16 $\mu\text{g/ml}$ of amphotericin B was required to attain a similar level of effectiveness against the diploid biofilm (Fig. 3A). Furthermore, CFU analysis also revealed that the haploid biofilm was less tolerant to amphotericin B than the diploid biofilm. At the amphotericin B concentration of 32 $\mu\text{g/ml}$, GZY803 haploids showed a 10-fold reduction of the persister population *i.e.* 0.1% *versus* 1%, as compared with the diploids (Fig. 3B). Taken together, our data showed that

the haploid biofilm is less tolerant to amphotericin B than the diploid biofilm.

Identification of AHP1 as a Critical Determinant of C. albicans Haploid Biofilm's Persistence Against Amphotericin B—Amphotericin B is known to exert its antifungal effect via binding to ergosterol, causing pore formation and cell death via increased oxidative stress (29, 30). Previously, we have shown that higher antioxidant capacity is important for higher resistance in *C. albicans* biofilms (31). Therefore, we further analyzed the haploid and diploid biofilm proteomes of *C. albicans* with respect to antioxidant proteins in order to find an explanation for the differential susceptibility to amphotericin B. Proteomics analysis identified Ahp1, a cell wall peroxidase (32) that plays a vital role in oxidative stress response, whose expression was lower in the haploid biofilm proteome (supplemental Table S3). Subsequent Western blot and real-time PCR analyses corroborated that the haploid biofilm expressed a significantly less amount of *AHP1* than the diploid biofilm at both mRNA and protein levels (Fig. 4A and 4B).

Antioxidant capacity is crucial for *C. albicans* to neutralize oxidative stress (33, 34). We hypothesized that the reduced *AHP1* expression found in the haploid biofilm might have caused a significant drop of the antioxidant potential, which contributes to the higher susceptibility to amphotericin B. To test this hypothesis, we expressed *AHP1* under the control of

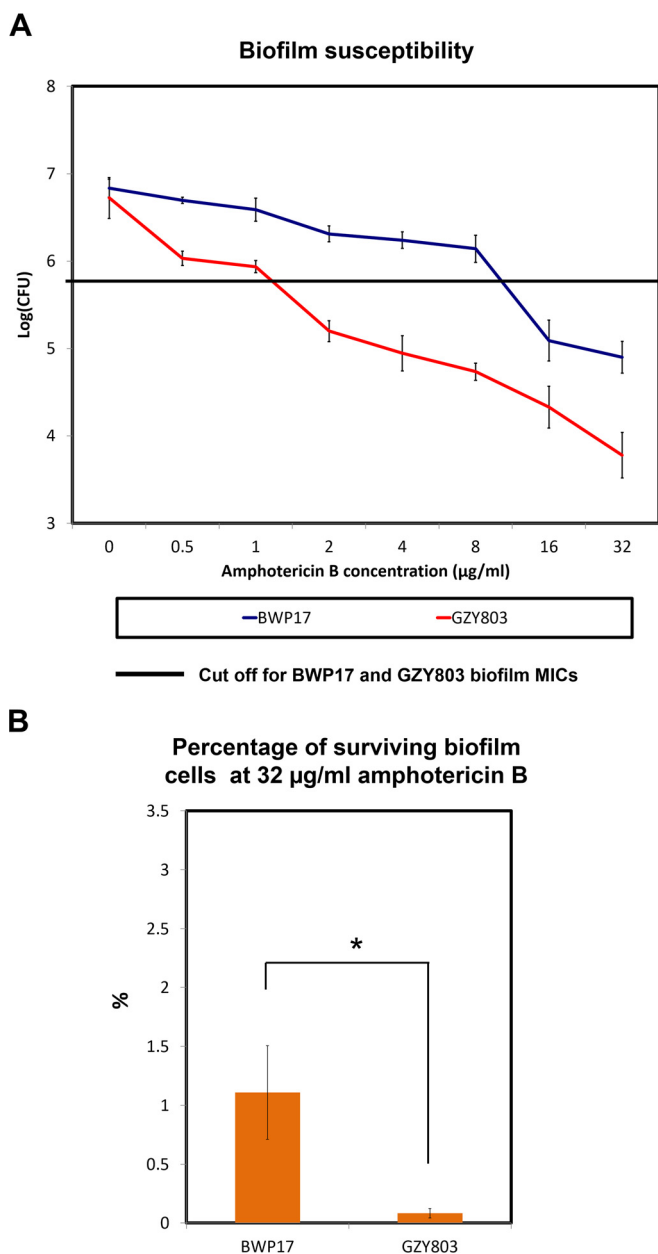


FIG. 3. GZY803 mature biofilm showed increased susceptibility to amphotericin B as compared with that of BWP17. *A*, *C. albicans* diploid (BWP17) and haploid (GZY803) strains were cultured at 30 °C in GMM (supplemented with required amino acids). Overnight cultures were then used to inoculate and allow biofilm development at 37 °C. Seventy-two-hour biofilms were treated with different concentrations of amphotericin B in RPMI for 24 h and minimum inhibition concentrations were recorded using CFU assays. *B*, Percentage of surviving biofilm cells at 32 µg/ml was also estimated by comparing the CFU at 32 µg/ml to the fungal count of untreated biofilms. Mean of at least three replicates is shown, with error bars showing S.D. (*): p value < 0.05.

the TetOff promoter in the GZY803 background (GZY1163) and examined the susceptibility to amphotericin B. In GZY1163, *AHP1* is overexpressed in the absence and shut down in the presence of doxycycline (20 µg/ml) (35). With or

without *AHP1* expression, the GZY1163 biofilm showed the same MIC (2 µg/ml) as the GZY803 biofilm (Fig. 4C). Interestingly, with *AHP1* overexpression (Dox-), the GZY1163 biofilm displayed a higher survival rate at higher concentrations of amphotericin B than the GZY803 biofilm (Fig. 4C and 4D). Approximately 10-fold higher survival rates were recorded in the GZY1163 biofilm under Dox- conditions at amphotericin B concentrations of 32 µg/ml (Fig. 4D). Adding doxycycline to the GZY1163 cells abolished the increased tolerance (Fig. 4D). Increased *AHP1* expression, therefore, seemed to augment the persister population and enhance *C. albicans* survival in the haploid biofilm to a level near the BWP17 diploid biofilm. Also, we noted that the GZY803 haploid biofilm showed reduced antioxidant capability than the diploid BWP17 biofilm. Overexpression of *AHP1* in the GZY803 background significantly improved the antioxidant potential in the biofilm (Fig. 4E). In summary, *AHP1* overexpression in GZY803 correlates well with the increased total antioxidant potential in biofilms and the tolerance against amphotericin B.

ahp1Δ/Δ C. albicans Biofilms Exhibited Reduced Persister Population and Increased Susceptibility to Amphotericin B—Preceding experiments revealed the critical contribution of *AHP1* in the persister population of *C. albicans* haploid biofilms. To examine whether *AHP1* plays the same role in diploid *C. albicans*, we generated the *ahp1Δ/Δ* mutant in the BWP17 background and assessed its biofilm formation and susceptibility to amphotericin B. Our XTT assays and CFU counts indicated that the *ahp1Δ/Δ* strain was capable of forming mature biofilm with a similar biomass as BWP17 (Fig. 5A and 5B). Despite comparable biomass, *ahp1Δ/Δ* biofilms displayed a lower antioxidant potential than BWP17 (Fig. 5C). Also, the CFU assays reflected a decrease in amphotericin B resistance in *ahp1Δ/Δ* biofilms (Fig. 5D). The MIC of *ahp1Δ/Δ* biofilms was reduced to 4 µg/ml, 4-fold lower than that of the BWP17 biofilms (16 µg/ml) (Fig. 5D). The persister population was also consistently reduced to 0.1% in the *ahp1Δ/Δ* biofilm as compared with 1% in that of BWP17 under 32 µg/ml amphotericin B treatment (Fig. 5E). These results corroborated findings in the haploids and confirmed *Ahp1*'s regulatory role in biofilm persister formation and tolerance against amphotericin B.

ira2Δ/Δ C. albicans Biofilms Displayed an Increased Susceptibility to Amphotericin B—Previously, we demonstrated that *Ira2* regulates biofilm formation in *C. albicans*. *IRA2* deletion was associated with defective biofilms characterized by reduced structural complexity (13). Next, we queried whether the *ira2Δ/Δ* biofilm is associated with reduced antifungal susceptibility like the *ahp1Δ/Δ* biofilm. Spot plate assays showed that *ira2Δ/Δ* biofilms exhibited increased susceptibility to amphotericin B but not to other antifungals (supplemental Fig. S4). The higher susceptibility of the *ira2Δ/Δ* biofilms to amphotericin B was confirmed by CFU assays (Fig. 6). The *ira2Δ/Δ* biofilms showed an MIC of 2 µg/ml whereas reintroducing *IRA2* into the deletion strain restored the resistance (MIC = 8 µg/ml). Hence,

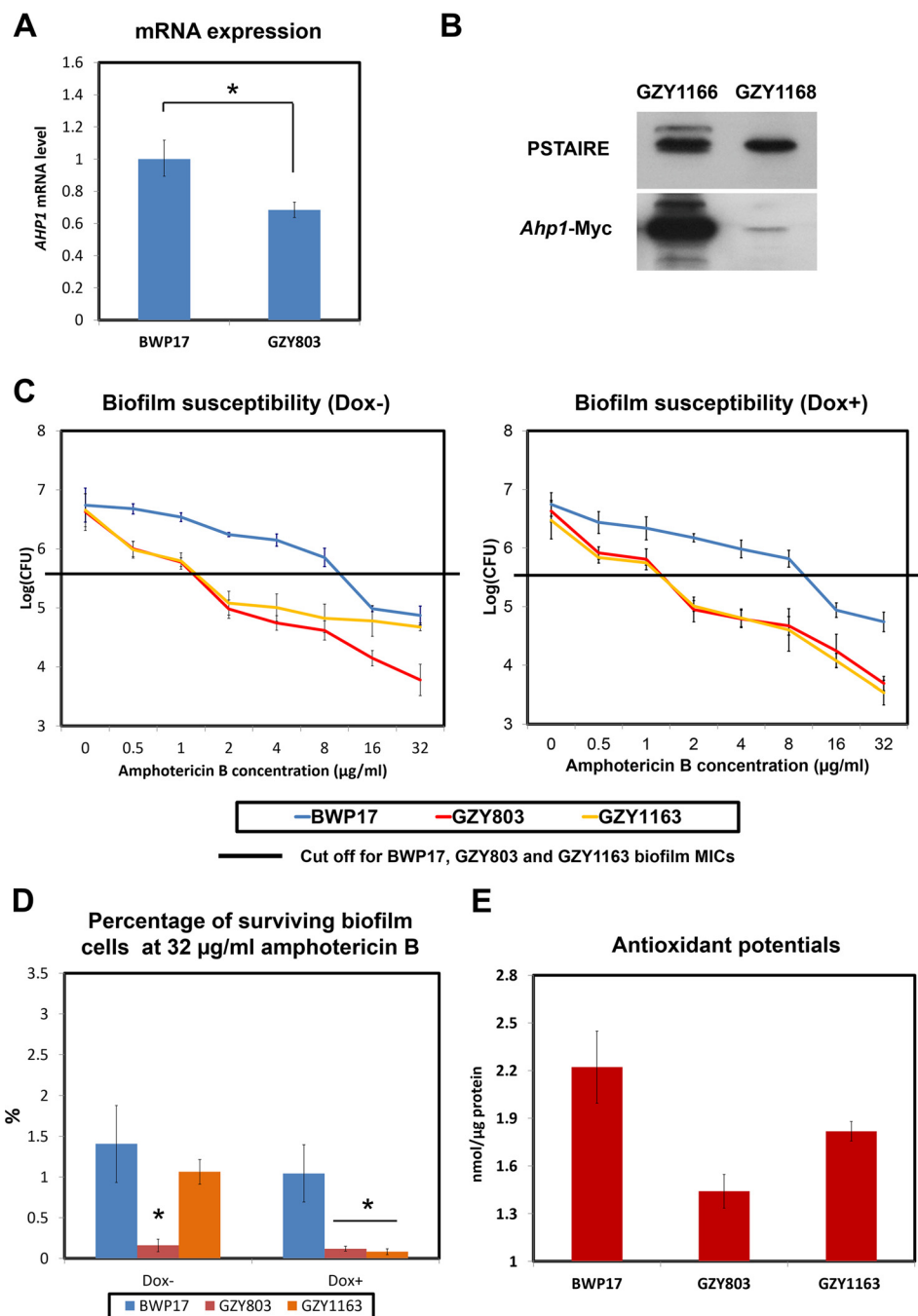


FIG. 4. Reduction of *AHP1* expression in GZY803 biofilms is linked with decreased antioxidant potentials and tolerance of amphotericin B. A, BWP17 and GZY803 cells were cultured in GMM supplemented with required amino acids. Overnight cultures were used to inoculate and allow biofilm development at 37 °C. RNA from 72-h biofilms was extracted and examined for *AHP1* expression using real-time PCR. *ACT1* and *PMA1* were used as controls. B, GZY1166 (BWP17:*AHP1*-Myc) and GZY1168 (GZY803:*AHP1*-Myc) were cultured in GMM supplemented with required amino acids. Overnight cultures were used to inoculate and allow biofilm development at 37 °C. Proteins from 72-h biofilm cells were extracted and examined for *AHP1* expression by Western blot. C, To examine amphotericin B resistance and tolerance relating to *AHP1* expression in the haploid biofilm, 72-h biofilms of GZY1163 (GZY803+Tetoff-Myc-*AHP1*) were treated with different concentrations of amphotericin B (in the presence or absence of 20 µg/ml of Dox) in RPMI for 24 h and CFUs were recorded. D, Percentage of surviving biofilm cell population at 32 µg/ml amphotericin B was also estimated following CFU assay. Diploid strain (BWP17) and haploid parent strain (GZY803) strain were included as controls. E, To estimate total antioxidant capacity, proteins from 72-h biofilms of BWP17, GZY803 and GZY1163 were also used for the antioxidant test. For all graphs, the mean of at least three replicates is shown, with error bars showing S.D. (*): *p* value <0.05.

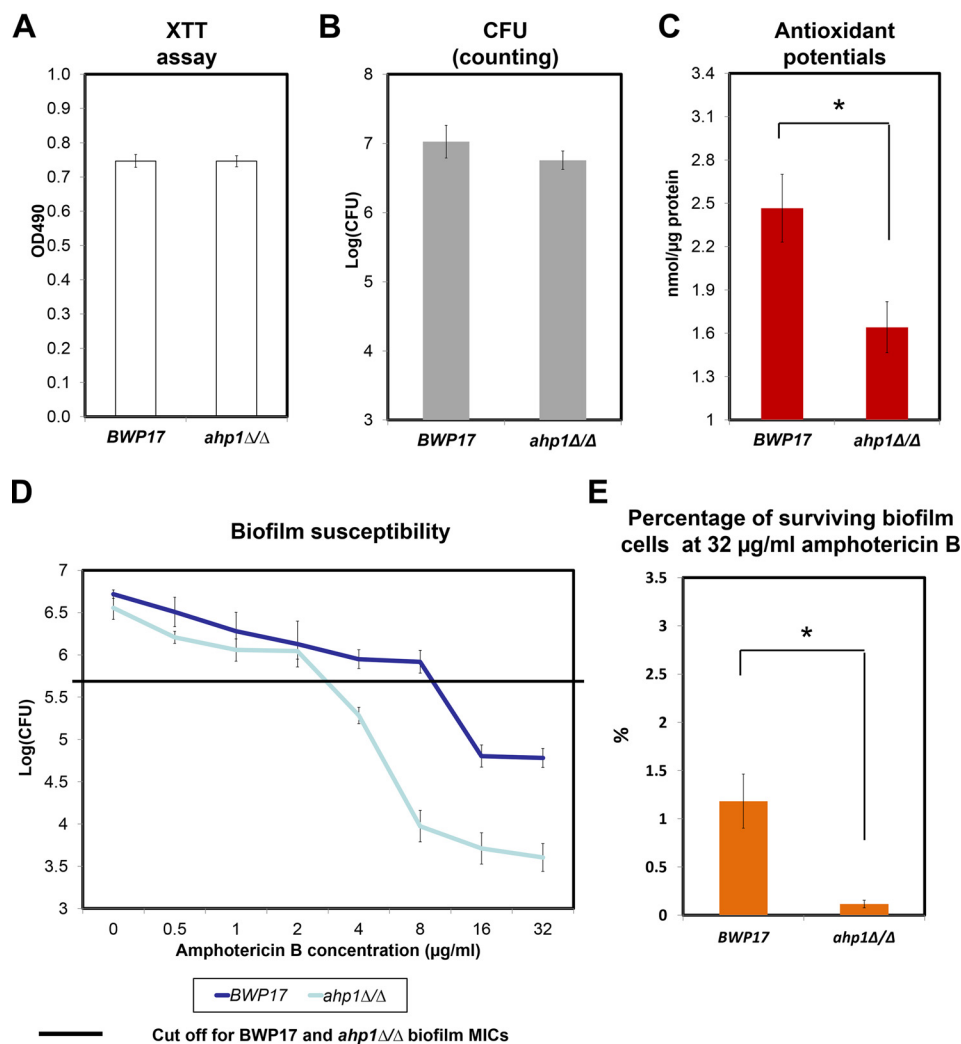


FIG. 5. *C. albicans ahp1*Δ/Δ biofilm exhibited reduced antioxidant potentials and diminished tolerance and resistance to amphotericin B. The overnight culture of *ahp1*Δ/Δ (GZY1210) *C. albicans* strain in GMM (supplemented with amino acids) was used inoculate and allow biofilm development at 37 °C. A, B, Quantification of biofilms formed by BWP17 and *ahp1*Δ/Δ after 72 h was conducted via XTT and CFU methods. C, Proteins from 72-h biofilms of BWP17 and *ahp1*Δ/Δ were also extracted and used to estimate the total antioxidant capacity. D, To examine amphotericin B resistance and tolerance, 72-h biofilm samples of BWP17 and *ahp1*Δ/Δ were treated with different concentrations of amphotericin B in RPMI for 24 h and CFUs were counted by plating the biofilm samples at each concentration on Sabouraud dextrose agar. E, Percentage of surviving biofilm cells at 32 μg/ml was also estimated by comparing the CFUs at 32 μg/ml to the fungal count of untreated biofilms. For all graphs, mean of at least three replicates is shown, with error bars showing S.D. (*): *p* value < 0.05.

the data demonstrated an association between *IRA2* and amphotericin B susceptibility of *C. albicans*.

As presented above, the first set of experiments derived from the comparative analysis of the proteomes of *C. albicans* haploid and diploid strains demonstrated that Ahp1 plays a pivotal role in the persister population of *C. albicans* biofilms against amphotericin B. The second set of experiments showed an association of *Ira2* with amphotericin B susceptibility in *C. albicans* biofilms. We also found that *IRA2* deletion results in lower expression of *AHP1* at the transcriptional level (Fig. 7A). We next asked whether overexpression of *AHP1* could protect the *ira2*Δ/Δ biofilm against amphotericin B and found that *AHP1* overexpression in the *ira2*Δ/Δ strain

(GZY1162) enhanced the tolerance of the *ira2*Δ/Δ biofilm against amphotericin B (Fig. 7B), leading to more than 10-fold increase in the survival rate under 16 μg/ml and 32 μg/ml amphotericin B treatments as compared with the *ira2*Δ/Δ strain (Fig. 7B); and shutting down the *AHP1* overexpression with doxycycline treatment abolished the increment in the persister population and drug tolerance of the GZY1162 biofilm (Fig. 7B). In addition, the diminished antioxidant capacity in the *ira2*Δ/Δ strain was largely restored when *AHP1* was overexpressed as compared with the BWP17 biofilm (Fig. 7C). Taken together, the comprehensive set of data firmly demonstrated a central role for Ahp1 in *Ira2*-mediated *C. albicans* biofilm's susceptibility to amphotericin B.

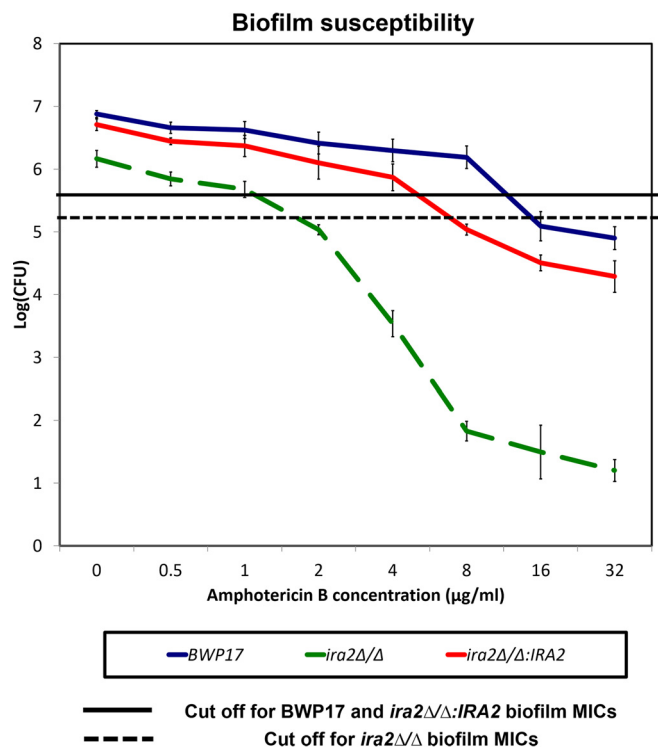


Fig. 6. *C. albicans ira2Δ/Δ* biofilm showed increased susceptibility to amphotericin B. *ira2Δ/Δ* (GZY923) *C. albicans* strain was cultured in GMM supplemented with required amino acids. The overnight culture was used to inoculate and allow biofilm development at 37 °C. Seventy-two-hour biofilms were treated with different concentrations of amphotericin B in RPMI for 24 h and CFUs were recorded by plating the biofilm samples at each concentration on Sabouraud dextrose agar. Parent strain (BWP17) and *ira2Δ/Δ* rescued strain (*ira2Δ/Δ:IRA2*, GZY1022) were included as controls. For all graphs, mean of at least three replicates is shown, with error bars showing S.D.

DISCUSSION

The recent discovery of haploid strains of *C. albicans* and subsequent validation of a haploid biofilm model has offered a new toolbox necessary for genetic manipulation in *C. albicans* research (13). In this study, we performed a comparative proteomics analysis on haploid and diploid *C. albicans* biofilms and targeted gene expression study to uncover *AHP1* as a pivotal antioxidant for the survival of persister cells against amphotericin B.

C. albicans haploid biofilm proteome shares a high similarity with that of the diploid biofilm with more than 70% of proteins expressed approximately at the same level, in particular that of structural proteins (Fig. 2). The high similarity explains our observation of haploid biofilms which comprised of comparable stacked yeast and hyphal cells encased in extracellular matrix as diploid biofilms (13). Expressions of proteins related to major biochemical pathways were considerably similar between haploid and diploid biofilms proteomes consistent with the comparable nature of the biofilms (Fig. 2).

On the other hand, some of the proteins were differentially expressed between the haploid and diploid biofilm pro-

teomes. The haploid biofilms expressed a higher level of key molecules in ATP synthesis and respiration such as citrate synthase and ATP synthase subunits (Fig. 2 and supplemental Table S2). On the contrary, the diploid biofilms exhibited an increase in proteins from the glycolysis pathway (36) including hexokinase, phosphofructokinase, and pyruvate kinase as haploids. These implied that haploid biofilms might rely more on fermentation and less aerobic respiration and glycolysis to generate ATP as compared with diploid biofilms. The haploid biofilms also demonstrated increased expression of chorismate synthase and aspartate semialdehyde dehydrogenase, determinant proteins in dicarboxylic and aromatic amino acids metabolisms (37, 38). Also, compared with the diploids, the haploid biofilm proteome exhibited a reduction in the expression of ribosome structure proteins. Depletion in ribosome generation and reduced glycolysis are consistent with the reported delay in growth, development, and maturation in *C. albicans* haploid biofilms as compared with the diploids (13). Proteomic analysis of the haploid biofilms also revealed a diminished expression of molecules in cell wall composition (Fig. 2 and supplemental Table S2), which correlates with reduced *in vivo* virulence in mouse models of infection (10) and delayed *ex vivo* invasion in oral tissue models (13). Among the identified cell wall proteins, alkyl hydroperoxide reductase 1 (Ahp1) and coproporphyrinogen III oxidase have previously been shown to be associated with antifungal resistance (31, 39–41). Overexpression of the coproporphyrinogen III oxidase, an enzyme of heme biosynthesis pathway, is a survival strategy of *Aspergillus fumigatus* and *Saccharomyces cerevisiae* against antifungal treatment (40, 41). On the other hand, our previous study on *C. albicans* biofilm proteome found that Ahp1 is associated with the higher antioxidative capacity of the *C. albicans* biofilms (8). Therefore, in the present study, we aimed to comprehensively investigate the role of Ahp1 in antifungal susceptibility of *C. albicans* biofilms.

The haploid cells in biofilm mode exhibited high resistance to the many antifungals tested (caspofungin, fluconazole, ketoconazole, and voriconazole) as the diploid biofilm. Intriguingly, we found that the haploid biofilms, having an MIC value of 2 µg/ml, are more susceptible to amphotericin B as compared with the diploid biofilms with an MIC of 16 µg/ml (Fig. 3). Different mechanisms that have been explored to explain the higher drug resistance of *C. albicans* biofilms include the presence of the extracellular polymeric substance (EPS), higher antioxidative capacity, and persister populations (5, 9, 42). However, we have observed that the *C. albicans* haploids form comparable biofilms with the extracellular matrix similar to diploid biofilms (13). Therefore, EPS is unlikely the explanation of the observed difference in amphotericin B susceptibility between the haploid and diploid biofilms. Other studies in the literature corroborated that EPS may not be a contributory factor against amphotericin B in *Candida* biofilms (43, 44).

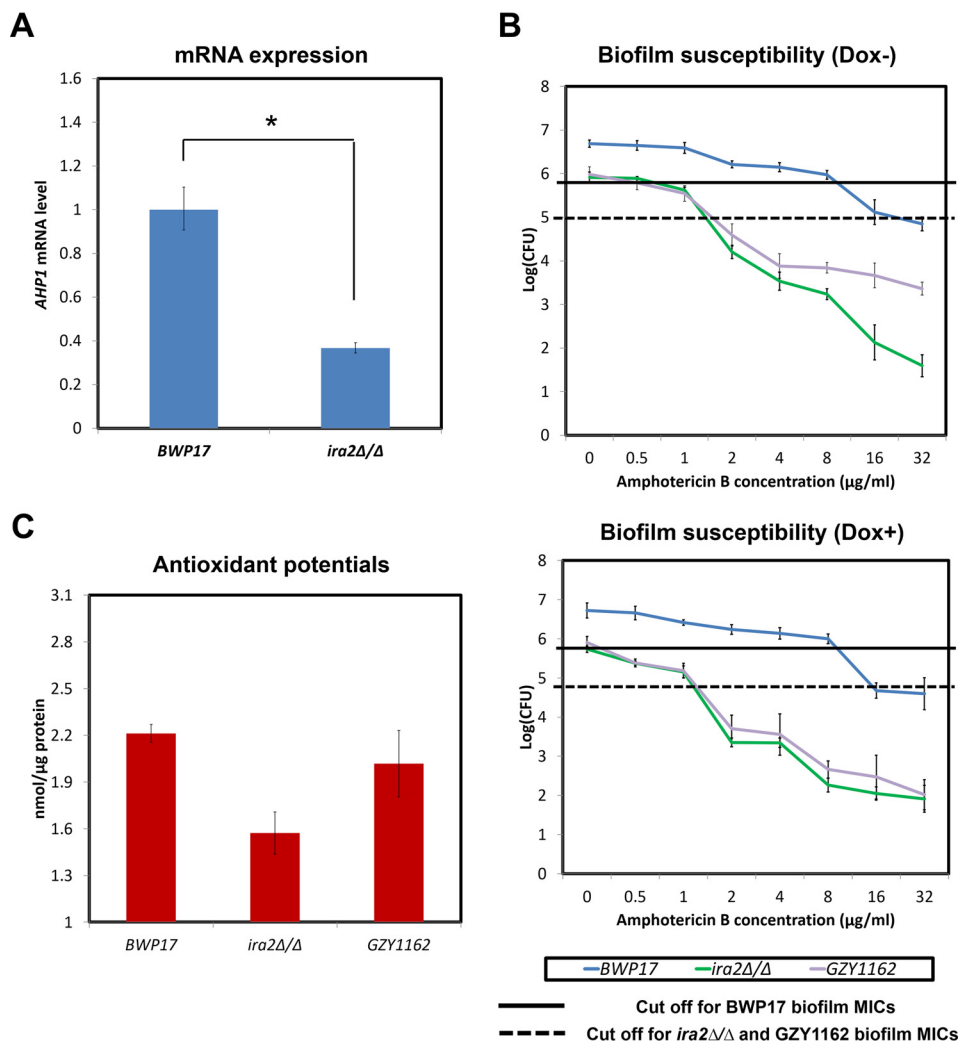


FIG. 7. IRA2 regulation of AHP1 is linked with *C. albicans* biofilms' antioxidant potentials and tolerance of amphotericin B. A, *ira2Δ/Δ* (GZY923) *C. albicans* strain was cultured in GMM supplemented with required amino acids. The overnight culture was used to inoculate and allow biofilm development at 37 °C. RNA from 72-h biofilm cells was extracted and examined for AHP1 expression using real-time PCR. ACT1 and PMA1 were used as controls. B, To examine amphotericin B resistance and tolerance, 72-h biofilms of BWP17, *ira2Δ/Δ* and *ira2Δ/Δ*+TetOff-Myc-AHP1 (GZY1162) were treated with different concentrations of amphotericin B (in the presence or absence of 20 μg/ml of Dox) in RPMI for 24 h and CFUs were recorded by plating the biofilm samples at each concentration on Sabouraud dextrose agar. C, To estimate total antioxidant capacity, proteins from 72-h biofilms of BWP17, *ira2Δ/Δ* and *ira2Δ/Δ*+TetOff-Myc-AHP1 (GZY1162) were also used for the antioxidant test. For all graphs, mean of at least three replicates is shown, with error bars showing S.D. (*): p value <0.05.

Another explanation for higher antifungal tolerance of the *C. albicans* biofilms is the subpopulation of cells called “persisters,” which are tolerant to repeated exposure to high concentration of antifungals (7). We observed that 0.1% of the cells in the haploid GZY803 biofilms survived at 32 μg/ml amphotericin B treatments whereas the diploid BWP17 biofilm had a 1% persister population (p value < 0.05). Hence, the haploid *C. albicans* possessed considerably fewer persister cells against amphotericin B than the diploids in biofilms (Fig. 3). To understand the differential behavior of the haploid and diploid biofilms, we examined the biofilm proteomes. The proteomics analysis demonstrated that the haploid biofilm has considerably less amount of Ahp1 (Fig. 4 and supplemental Table S3),

a key protein of the antioxidant defense system, located in the cell wall (33). Ahp1 is a member of the peroxiredoxin family and plays a vital role in protecting the cells from reactive oxygen species as well as in stress adaptation (32). Ahp1 coordinates with other peroxidases such as Trx1 to protect the cells against oxidative stress (45). Hence, upon binding to its substrate, Ahp1 induces antioxidant response by activating the Cad1 transcriptional signaling pathway (46). Moreover, previous studies have shown that Ahp1 is an important antioxidant in the *C. albicans* biofilms (31, 47). These are particularly relevant in antifungals like amphotericin B that is known to generate reactive oxidative species (30, 48). Foregoing analysis provided clear evidence on the role of Ahp1 and

antioxidant responses in the persister population of *C. albicans* biofilms against amphotericin B treatment. Our findings corroborate with previous works. Superoxide dismutases, important players in *C. albicans* antioxidant defense, were found to be associated with biofilm persistence to miconazole (16). Not only in fungi, hydrogen peroxide-inducible genes activator (*OxyR*), a sensor of hydrogen peroxide, was also shown as a determinant of bacterial persisters (49). Our study, therefore, has emphasized the crucial contribution of antioxidant protection in survival strategy against antifungal treatment.

We also found a link between *IRA2* and *AHP1* in amphotericin B resistance of *C. albicans* biofilms. *Ira2* is a putative GTPase-regulating protein of Ras1, an activator of the cAMP/protein kinase A pathway (50). *Ira2* is known to mediate fungal heat shock and stress response (51). Previously, we demonstrated that *Ira2* regulates biofilm formation in *C. albicans* and a strain lacking *IRA2* formed a thinner and less dense biofilm than wild-type strains (13). Here, we found that despite the structural defects, *ira2Δ/Δ* biofilms remain resistant to several antifungals but more susceptible to amphotericin B than the wild-type strain (Fig. 6 and supplemental Fig. S4). Therefore, we assumed that the persister population of *ira2Δ/Δ* biofilms lacked some elements required for survival against amphotericin B treatment. Our subsequent experiments uncovered hitherto a previously unknown link between *AHP1* and *IRA2* in *C. albicans* biofilms (Fig. 7). *AHP1* expression in *C. albicans* persister population could be directly or indirectly regulated by *Ira2*. It has been shown that *AHP1* is regulated by *Yap1* and *Skn7* (45). Interestingly, functions of both *Yap1* and *Skn7* are linked to GTPase molecules. In *Saccharomyces cerevisiae*, *Skn7* is known to interact with Rho GTPases (52). On the other hand, *ScYap1* translocation to the cytoplasm is required for the *Ran* GTPase activity (53). *Ira2* is a regulator of Ras (51) which belongs to the superfamily of small GTPases including Rho and Ran (54). Therefore, it is possible that *Ira2* is a direct or indirect upstream effector of Ran and Rho GTPases, which in turn regulates *Skn7* and *Yap1* and finally mediates *AHP1* expression.

In conclusion, the present study, for the first time, unraveled the comparative ploidy proteome of haploid and diploid *C. albicans* biofilms. Subsequent studies on haploid mutagenesis provided new molecular insights to explain the higher resistance of *C. albicans* biofilms against amphotericin B, the gold standard antifungal agent. Taken together, we demonstrated that *IRA2*'s role in biofilm regulation is related to that of *AHP1*, both increase the antioxidative capacities and survival rates of *C. albicans* cells in the biofilm under amphotericin B treatment. These findings will open up new avenues to develop targeted therapy to eradicate the persister population in *C. albicans* biofilms, which could benefit millions of patients suffering from biofilm-associated infections.

Acknowledgments—The mass spectrometry proteomics data have been deposited to the ProteomeXchange Consortium via the PRIDE (55) partner repository with the data set identifier PXD004274.

* This study was supported by NMRC-NIG (R-221-000-073-511), NUS-Start-up (R-221-000-064-133) to C.J.S. and funding from Agency for Science, Technology, and Research (A*STAR) to Y.W.

§ This article contains supplemental material.

|| These authors contributed equally to this work.

** To whom correspondence may be addressed: Oral Sciences, Faculty of Dentistry, National University of Singapore, 11 Lower Kent Ridge Road, Singapore 119083. Tel.: (+65) 6779 5555; Fax: (+65) 6778 5742; E-mail: jaya@nus.edu.sg. Or, Institute of Molecular and Cell Biology, Agency for Science, Technology and Research, Proteos, Biopolis Drive, Singapore 138673. Tel.: (+65) 65869521; Fax: (+65) 67791117, E-mail: mcbwangy@imcb.a-star.edu.sg.

REFERENCES

- Mavor, A. L., Thewes, S., and Hube, B. (2005) Systemic fungal infections caused by *Candida* species: epidemiology, infection process and virulence attributes. *Curr. Drug Targets* **6**, 863–874
- Gullo, A. (2009) Invasive fungal infections: the challenge continues. *Drugs* **69**, 65–73
- Delaloye, J., and Calandra, T. (2014) Invasive candidiasis as a cause of sepsis in the critically ill patient. *Virulence* **5**, 161–169
- Wisplinghoff, H., Bischoff, T., Tallent, S. M., Seifert, H., Wenzel, R. P., and Edmond, M. B. (2004) Nosocomial bloodstream infections in US hospitals: analysis of 24,179 cases from a prospective nationwide surveillance study. *Clin. Infect. Dis.* **39**, 309–317
- Seneviratne, C. J., Jin, L., and Samaranyake, L. P. (2008) Biofilm lifestyle of *Candida*: a mini review. *Oral Diseases* **14**, 582–590
- Ramage, G., Saville, S. P., Thomas, D. P., and Lopez-Ribot, J. L. (2005) *Candida* biofilms: an update. *Eukaryotic Cell* **4**, 633–638
- LaFleur, M. D., Kumamoto, C. A., and Lewis, K. (2006) *Candida albicans* biofilms produce antifungal-tolerant persister cells. *Antimicrobial Agents Chemother.* **50**, 3839–3846
- Chandra, J., Kuhn, D. M., Mukherjee, P. K., Hoyer, L. L., McCormick, T., and Ghannoum, M. A. (2001) Biofilm formation by the fungal pathogen *Candida albicans*: development, architecture, and drug resistance. *J. Bacteriol.* **183**, 5385–5394
- Mathe, L., and Van Dijk, P. (2013) Recent insights into *Candida albicans* biofilm resistance mechanisms. *Curr. Genet.* **59**, 251–264
- Hickman, M. A., Zeng, G., Forche, A., Hiraakawa, M. P., Abbey, D., Harrison, B. D., Wang, Y. M., Su, C. H., Bennett, R. J., Wang, Y., and Berman, J. (2013) The 'obligate diploid' *Candida albicans* forms mating-competent haploids. *Nature* **494**, 55–59
- Sarosi, G. A. (1990) Amphotericin B. Still the 'gold standard' for antifungal therapy. *Postgrad Med.* **88**, 151–152, 155–161, 165–166
- Zeng, G., Wang, Y. M., Chan, F. Y., and Wang, Y. (2014) One-step targeted gene deletion in *Candida albicans* haploids. *Nat. Protoc.* **9**, 464–473
- Seneviratne, C. J., Zeng, G., Truong, T., Sze, S., Wong, W., Samaranyake, L., Chan, F. Y., Wang, Y. M., Wang, H., Gao, J., and Wang, Y. (2015) New "haploid biofilm model" unravels *IRA2* as a novel regulator of *Candida albicans* biofilm formation. *Sci. Reports* **5**, 12433
- Seneviratne, C. J., Jin, L. J., Samaranyake, Y. H., and Samaranyake, L. P. (2008) Cell density and cell aging as factors modulating antifungal resistance of *Candida albicans* biofilms. *Antimicrobial Agents Chemother.* **52**, 3259–3266
- National Committee for Clinical Laboratory Standards. (2002) Reference method for broth dilution antifungal susceptibility testing of yeasts—second edition: Approved standard M27-A2. *Natl. Comm. Clin. Lab. Standards* Wayne, PA
- Bink, A., Vandenbosch, D., Coenye, T., Nelis, H., Cammue, B. P., and Thevissen, K. (2011) Superoxide dismutases are involved in *Candida albicans* biofilm persistence against miconazole. *Antimicrobial Agents Chemother.* **55**, 4033–4037
- Vylkova, S., Jang, W. S., Li, W., Nayyar, N., and Edgerton, M. (2007) Histatin 5 initiates osmotic stress response in *Candida albicans* via activation of the Hog1 mitogen-activated protein kinase pathway. *Eukaryotic Cell* **6**, 1876–1888
- Ghosh, D., Li, Z., Tan, X. F., Lim, T. K., Mao, Y., and Lin, Q. (2013) iTRAQ based quantitative proteomics approach validated the role of calcyclin binding protein (CacyBP) in promoting colorectal cancer metastasis.

- Mol. Cell. Proteomics* **12**, 1865–1880
19. Gan, C. S., Chong, P. K., Pham, T. K., and Wright, P. C. (2007) Technical, experimental, and biological variations in isobaric tags for relative and absolute quantitation (iTRAQ). *J. Proteome Res.* **6**, 821–827
 20. Eisen, M. B., Spellman, P. T., Brown, P. O., and Botstein, D. (1998) Cluster analysis and display of genome-wide expression patterns. *Proc. Natl. Acad. Sci. U.S.A.* **95**, 14863–14868
 21. Shannon, P., Markiel, A., Ozier, O., Baliga, N. S., Wang, J. T., Ramage, D., Amin, N., Schwikowski, B., and Ideker, T. (2003) Cytoscape: a software environment for integrated models of biomolecular interaction networks. *Genome Res.* **13**, 2498–2504
 22. Maere, S., Heymans, K., and Kuiper, M. (2005) BiNGO: a Cytoscape plugin to assess overrepresentation of gene ontology categories in biological networks. *Bioinformatics* **21**, 3448–3449
 23. Li, P., Seneviratne, C. J., Alpi, E., Vizcaino, J. A., and Jin, L. (2015) Delicate Metabolic Control and Coordinated Stress Response Critically Determine Antifungal Tolerance of *Candida albicans* Biofilm Persists. *Antimicrobial Agents Chemother.* **59**, 6101–6112
 24. Wiese, S., Reidegeld, K. A., Meyer, H. E., and Warscheid, B. (2007) Protein labeling by iTRAQ: a new tool for quantitative mass spectrometry in proteome research. *Proteomics* **7**, 340–350
 25. Gao, Y., Lim, T. K., Lin, Q., and Li, S. F. (2016) Identification of cypermethrin induced protein changes in green algae by iTRAQ quantitative proteomics. *J. Proteomics* **139**, 67–76
 26. Lunt, S. Y., and Vander Heiden, M. G. (2011) Aerobic glycolysis: meeting the metabolic requirements of cell proliferation. *Annu. Rev. Cell Dev. Biol.* **27**, 441–464
 27. Vander Heiden, M. G., Cantley, L. C., and Thompson, C. B. (2009) Understanding the Warburg effect: the metabolic requirements of cell proliferation. *Science* **324**, 1029–1033
 28. Chaffin, W. L., Lopez-Ribot, J. L., Casanova, M., Gozalbo, D., and Martinez, J. P. (1998) Cell wall and secreted proteins of *Candida albicans*: identification, function, and expression. *Microbiol. Mol. Biol. Rev.* **62**, 130–180
 29. Mitri, S., Xavier, J. B., and Foster, K. R. (2011) Social evolution in multispecies biofilms. *Proc. Natl. Acad. Sci. U.S.A.* **108**, 10839–10846
 30. Mesa-Arango, A. C., Trevijano-Contador, N., Roman, E., Sanchez-Fresneda, R., Casas, C., Herrero, E., Arguelles, J. C., Pla, J., Cuenca-Estrella, M., and Zaragoza, O. (2014) The production of reactive oxygen species is a universal action mechanism of Amphotericin B against pathogenic yeasts and contributes to the fungicidal effect of this drug. *Antimicrobial Agents Chemother.* **58**, 6627–6638
 31. Seneviratne, C. J., Wang, Y., Jin, L., Abiko, Y., and Samaranayake, L. P. (2008) *Candida albicans* biofilm formation is associated with increased anti-oxidative capacities. *Proteomics* **8**, 2936–2947
 32. Chauhan, N., Inglis, D., Roman, E., Pla, J., Li, D., Calera, J. A., and Calderone, R. (2003) *Candida albicans* response regulator gene SSK1 regulates a subset of genes whose functions are associated with cell wall biosynthesis and adaptation to oxidative stress. *Eukaryotic Cell* **2**, 1018–1024
 33. Chauhan, N., Latge, J. P., and Calderone, R. (2006) Signalling and oxidant adaptation in *Candida albicans* and *Aspergillus fumigatus*. *Nat. Rev. Microbiol.* **4**, 435–444
 34. Dantas Ada, S., Day, A., Ikeh, M., Kos, I., Achan, B., and Quinn, J. (2015) Oxidative stress responses in the human fungal pathogen, *Candida albicans*. *Biomolecules* **5**, 142–165
 35. Park, Y. N., and Morschhauser, J. (2005) Tetracycline-inducible gene expression and gene deletion in *Candida albicans*. *Eukaryotic Cell* **4**, 1328–1342
 36. Wimhurst, J. M., and Manchester, K. L. (1973) Induction and suppression of the key enzymes of glycolysis and gluconeogenesis in isolated perfused rat liver in response to glucose, fructose and lactate. *Biochem. J.* **134**, 143–156
 37. Kitzing, K., Auweter, S., Amrhein, N., and Macheroux, P. (2004) Mechanism of chorismate synthase. Role of the two invariant histidine residues in the active site. *J. Biol. Chem.* **279**, 9451–9461
 38. Holland, M. J., and Westhead, E. W. (1973) Purification and characterization of aspartic -semialdehyde dehydrogenase from yeast and purification of an isozyme of glyceraldehyde-3-phosphate dehydrogenase. *Biochemistry* **12**, 2264–2270
 39. Gautam, P., Upadhyay, S. K., Hassan, W., Madan, T., Sirdeshmukh, R., Sundaram, C. S., Gade, W. N., Basir, S. F., Singh, Y., and Sarma, P. U. (2011) Transcriptomic and proteomic profile of *Aspergillus fumigatus* on exposure to artemisinin. *Mycopathologia* **172**, 331–346
 40. Gautam, P., Shankar, J., Madan, T., Sirdeshmukh, R., Sundaram, C. S., Gade, W. N., Basir, S. F., and Sarma, P. U. (2008) Proteomic and transcriptomic analysis of *Aspergillus fumigatus* on exposure to amphotericin B. *Antimicrobial Agents Chemother.* **52**, 4220–4227
 41. Zhang, L., Zhang, Y., Zhou, Y., An, S., Zhou, Y., and Cheng, J. (2002) Response of gene expression in *Saccharomyces cerevisiae* to amphotericin B and nystatin measured by microarrays. *J. Antimicrob. Chemother.* **49**, 905–915
 42. Seneviratne, C. J., Wang, Y., Jin, L., Wong, S. S., Herath, T. D., and Samaranayake, L. P. (2012) Unraveling the resistance of microbial biofilms: has proteomics been helpful? *Proteomics* **12**, 651–665
 43. Bailie, G. S., and Douglas, L. J. (2000) Matrix polymers of *Candida* biofilms and their possible role in biofilm resistance to antifungal agents. *J. Antimicrob. Chemother.* **46**, 397–403
 44. Hawser, S. P., and Douglas, L. J. (1995) Resistance of *Candida albicans* biofilms to antifungal agents in vitro. *Antimicrobial Agents Chemother.* **39**, 2128–2131
 45. Lee, J., Spector, D., Godon, C., Labarre, J., and Toledano, M. B. (1999) A new antioxidant with alkyl hydroperoxide defense properties in yeast. *J. Biol. Chem.* **274**, 4537–4544
 46. Iwai, K., Naganuma, A., and Kuge, S. (2010) Peroxiredoxin Ahp1 acts as a receptor for alkylhydroperoxides to induce disulfide bond formation in the Cad1 transcription factor. *J. Biol. Chem.* **285**, 10597–10604
 47. Sun, X., Lu, H., Jiang, Y., and Cao, Y. (2013) CalPF19998 reduces drug susceptibility by enhancing the ability of biofilm formation and regulating redox homeostasis in *Candida albicans*. *Curr. Microbiol.* **67**, 322–326
 48. Phillips, A. J., Sudbery, I., and Ramsdale, M. (2003) Apoptosis induced by environmental stresses and amphotericin B in *Candida albicans*. *Proc. Natl. Acad. Sci. U.S.A.* **100**, 14327–14332
 49. Wu, N., He, L., Cui, P., Wang, W., Yuan, Y., Liu, S., Xu, T., Zhang, S., Wu, J., Zhang, W., and Zhang, Y. (2015) Ranking of persister genes in the same *Escherichia coli* genetic background demonstrates varying importance of individual persister genes in tolerance to different antibiotics. *Front. Microbiol.* **6**, 1003
 50. Tanaka, K., Lin, B. K., Wood, D. R., and Tamanoi, F. (1991) IRA2, an upstream negative regulator of RAS in yeast, is a RAS GTPase-activating protein. *Proc. Natl. Acad. Sci. U.S.A.* **88**, 468–472
 51. Tanaka, K., Nakafuku, M., Tamanoi, F., Kaziro, Y., Matsumoto, K., and Toh-e, A. (1990) IRA2, a second gene of *Saccharomyces cerevisiae* that encodes a protein with a domain homologous to mammalian ras GTPase-activating protein. *Mol. Cell. Biol.* **10**, 4303–4313
 52. Alberts, A. S., Bouquin, N., Johnston, L. H., and Treisman, R. (1998) Analysis of RhoA-binding proteins reveals an interaction domain conserved in heterotrimeric G protein beta subunits and the yeast response regulator protein Skn7. *J. Biol. Chem.* **273**, 8616–8622
 53. Yan, C., Lee, L. H., and Davis, L. I. (1998) Crm1p mediates regulated nuclear export of a yeast AP-1-like transcription factor. *EMBO J.* **17**, 7416–7429
 54. Goitre, L., Trapani, E., Trabalzini, L., and Retta, S. F. (2014) The Ras superfamily of small GTPases: the unlocked secrets. *Methods Mol. Biol.* **1120**, 1–18
 55. Vizcaino, J. A., Csordas, A., del-Toro, N., Dianes, J. A., Griss, J., Lavidas, I., Mayer, G., Perez-Riverol, Y., Reisinger, F., Ternent, T., Xu, Q. W., Wang, R., and Hermjakob, H. (2016) 2016 update of the PRIDE database and its related tools. *Nucleic Acids Res.* **44**, D447–D456